

LUMO energy of model compounds of bispyridinium compounds as an index for the inhibition of choline kinase

Joaquín Campos^a, María del Carmen Núñez^a, Vicente Rodríguez^a, Antonio Entrena^a,
Rubén Hernández-Alcoceba^b, Félix Fernández^b, Juan Carlos Lacal^b, Miguel A. Gallo^a,
Antonio Espinosa^{a*}

^aDepartamento de Química Orgánica, Facultad de Farmacia, Campus de Cartuja s/n, E-18071 Granada, Spain

^bInstituto de Investigaciones Biomédicas, Consejo Superior de Investigaciones Científicas, c/ Arturo Duperier,
E-28029 Madrid, Spain

Received 2 October 2000; revised 2 December 2000; accepted 4 January 2001

Abstract – Eleven derivatives of 1,1'-[1,2-ethylenebis(benzene-1,4-diylmethylene)]bis(4-pyridinium) dibromides bearing various groups at C-4 of the pyridinium moiety were synthesized and examined for their inhibition of choline kinase (ChoK) and antiproliferative activities. The C-4 substituents include electron-releasing, neutral or electron-withdrawing groups. A one-parameter regression equation has been derived which satisfactorily describes the ex vivo inhibitory potency of ChoK of the title compounds. The electronic effect plays a critical function in the ex vivo inhibition of ChoK although the role of electrostatic interactions could be altered due to a solvation process of both ChoK and ligands. © 2001 Éditions scientifiques et médicales Elsevier SAS

antiproliferative agents / electrostatic effects / choline kinase / quantitative structure–activity relationship

1. Introduction

During the past 20 years, a variety of approaches has been made for cancer chemotherapy, and many antitumour drugs have been developed for clinical use. In the treatment of solid tumours, however, the conventional approaches have met with only limited success, and cancer still remains as one of the leading causes of human mortality. Current chemotherapeutic antitumour drugs suffer two major drawbacks: adverse effects and drug resistance. Adverse effects associated with conventional antitumour drugs are usually caused by their indiscriminate cytotoxic effect on nor-

mal cells. In drug resistance, the use of combination chemotherapy, which is the administration of several drugs with different and complementary mechanisms of action, is regarded as the more effective approach. Therefore, the object of our current research is to overcome the shortcomings of present cancer chemotherapy with an antitumour drug with a new mechanism of action, capable of discriminating tumour cells from normal proliferative cells and exhibiting selective toxicity against cancer.

As a new mechanism of action, we focused our attention on choline kinase (ChoK, EC 2.7.1.32). This enzyme is the first one in the cytidine 5'-diphosphate-choline pathway for the synthesis of phosphatidylcholine, and phosphorylates choline to phosphorylcholine (PCho) using adenosine 5'-triphosphate as the phosphate donor [1–3]. The *ras* oncogenes are mutated in about 25% of human tumours [4]. These genes encode 21 kDa proteins called p21 or Ras. In vitro studies of oncogenic Ras proteins, and products and growth factors have shown that

Abbreviations: ChoK, choline kinase; PCho, phosphorylcholine; MO, molecular orbital; AM1, Austin Model 1; QSAR, quantitative structure–activity relationship; HOMO, highest occupied molecular orbital; LUMO, lowest unoccupied molecular orbital; HF, Hartree–Fock; IPCM, isodensity surface polarized continuum model; IC₅₀, concentration resulting in 50% inhibition; PI3K, phosphatidylinositol 3'-kinase; PLD, phospholipase D; PI-PLC, phosphatidylinositol-phospholipase C; MAPK, mitogen-activated protein kinase.

* Corresponding author

E-mail address: aespinos@ugr.es (A. Espinosa).

phosphocholine contributes to cellular growth regulation and intracellular signal transduction. Ras proteins play a pivotal role in cellular signal transduction, and help regulate cellular proliferation and terminal differentiation [5–7]. NMR studies demonstrated that the levels of *PCho* were increased in a large number of tumour cells from mice and human beings when compared to their normal counterparts [8]. These events together with our results on symmetrical bisquaternary derivatives with increased inhibitory activity towards ChoK [9], and very recently, the *in vivo* antitumour activity of several ChoK inhibitors [10], provide strong support to the hypothesis of the important role of phosphatidylcholine metabolites in the regulation of normal cell growth and that its alteration is important for the establishment of cancer cells.

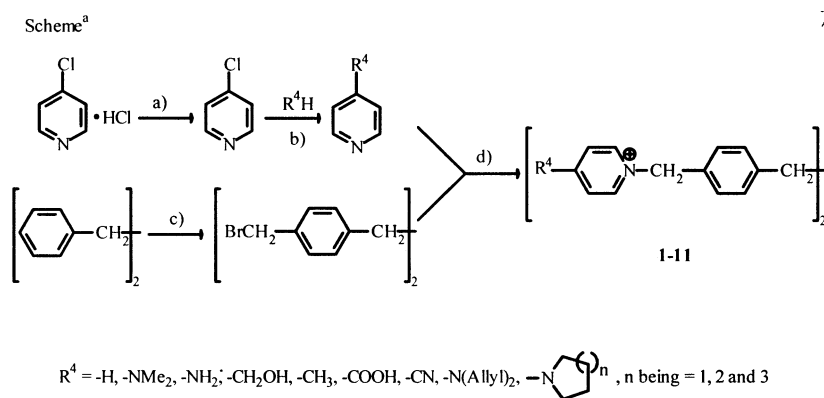
2. Chemistry

In this paper we have synthesized eleven symmetrical bispyridinium derivatives **1–11** (figure 1). The C-4 substituents of the pyridinium moiety include electron-withdrawing (strong ones like $-\text{C}\equiv\text{N}$ and $-\text{COOH}$), neutral ($-\text{H}$, $-\text{CH}_3$, $-\text{CH}_2\text{OH}$) or electron-releasing groups (the $-\text{NH}_2$ is a strong one, the $-\text{NMe}_2$ group is the most electron-releasing neutral substituent known [11], and the diallylamino, pyrrolidino, piperidino and perhydroazepino groups).

The compounds for this study were synthesized by reaction between the corresponding 4-substituted

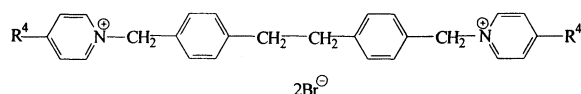
pyridines and bis-*p*-(bromomethyl)biphenyl [12] in butanone at 100°C in a sealed tube (figure 1). After filtration the products were recrystallized from EtOH/Et₂O, except **6** (MeOH/Et₂O). 4-(*N,N*-Diallylamino)pyridine [13] and 4-piperidinopyridine [14] were prepared as reported previously. 4-Perhydroazepinopyridine (89%) is a new compound and was obtained from 4-chloropyridine and the corresponding secondary amine according to the method used for 4-(*N,N*-diallylamino)pyridine [13]. All the new compounds gave satisfactory ¹H-NMR, ¹³C-NMR, and FABHRMS.

Although at first glance the NMR and mass spectra of compounds **1**, **2**, **4** and **6–11** looked clean, there were problems with their elemental analyses. Despite numerous recrystallizations from ethanol/diethyl ether, elemental analyses of **1** gave C and N values which were about 3.4 and 0.7% too low, indicating some water content. Nevertheless, H values were +0.2% of the theoretical values. The C, N values did not improve significantly when drying of the samples was carried out in high vacuum at 40°C instead of room temperature. Obviously, water can be trapped in **1**. These phenomena were also observed for compounds **2**, **4** and **6–11**. By adding the necessary amounts of water the elemental analyses concord perfectly (see Section 6). The physicochemical properties of compounds **1–11** are shown in table I. Later on, it will be discussed that water (in both aspects, as a reactive and as a solvent) plays a pivotal role in the biological behaviour of these bisquaternary compounds.



^a Methods: a) NaOH, 86 %; b) followed when R^4 = diallylamino, pyrrolidino, piperidino and perhydroazepino groups, reflux temperature, 34–95 %; c) see ref. 12; d) sealed tube, butanone, 100 °C, 37–94%.

Figure 1. Synthesis of bispyridinium derivatives.

Table I. Physicochemical properties for the symmetrical bispyridinium compounds **1–11**.

Compound	R ⁴	Formula ^a	Mp (°C)	Crystal solvent ^b	λ _{max} (nm)	ε	Yield ^c (%)
1	–NMe ₂	C ₃₀ H ₃₆ N ₄ Br ₂ ·2H ₂ O	291–293	a	293	35 100	48
2	–NH ₂	C ₂₆ H ₂₈ N ₄ Br ₂ ·0.2H ₂ O	295–296	a	272	5230	83
3	–CH ₂ OH	C ₂₈ H ₃₀ N ₂ O ₂ Br ₂	> 310	a	254	4940	63
4	–CH ₃	C ₂₈ H ₃₀ N ₂ Br ₂ ·H ₂ O	> 310	a	254	8470	75
5	–COOH	C ₂₈ H ₂₆ N ₂ O ₄ Br ₂	> 310	b	263	8340	59
6	–C≡N	C ₂₈ H ₂₄ N ₄ Br ₂ ·0.3H ₂ O	255–257	a	278	8980	84
7	–N(Allyl) ₂	C ₃₈ H ₄₄ N ₄ Br ₂ ·H ₂ O	^d	a	293	5030	37
8	–NC ₄ H ₈ ^e	C ₃₄ H ₄₀ N ₄ Br ₂ ·2H ₂ O	307–309	a	293	2640	80
9	–NC ₅ H ₁₀ ^f	C ₃₆ H ₄₄ N ₄ Br ₂ ·2.4H ₂ O	236–238	a	302	3580	70
10	–NC ₆ H ₁₂ ^g	C ₃₈ H ₄₈ N ₄ Br ₂ ·1.8H ₂ O	> 310	a	302	2590	94
11	–H	C ₂₆ H ₂₆ N ₂ Br ₂ ·1.5H ₂ O	109–110	a	257	8850	84

^a Satisfactory microanalyses obtained: C, H, N values are within ± 0.4% of the theoretical values.

^b Crystal solvent: a, ethyl alcohol/diethyl ether; b, methanol/diethyl ether.

^c Yield related to last step.

^d Very hygroscopic to determine its mp.

^e Pyrrolidino.

^f Piperidino.

^g Perhydroazepino.

3. Pharmacology

Compounds **1–11** were tested in an ex vivo system using purified ChoK from yeast (in a test tube without cells) as a target. This assay allowed us to evaluate the effect on **1–11** activities without considering the possible effects on other properties such as permeability into intact cells, specific cellular environments, putative intracellular modifications of the synthesized compounds or enzyme compartmentalization. The effects on cell proliferation by the ChoK inhibitors in *ras*-transformed cells were next investigated. The Hill equation was fitted to the data to obtain estimates of the IC₅₀.

4. Results and discussion

The electronic influence of R⁴ on **11** alters its charge distribution (data not shown) and molecular orbital (MO) energies. During the past three decades most of the QSARs derived for biological systems have relied on the use of Hammett-type σ constants to account for electronic variation associated with changes in molecular structure. As a result, these studies have often been limited to sets of congeners

that could be treated by using Hammett-type substituent constants. The conventional electronic parameters are available for only a relatively small number of substituents (e.g. σ_P and σ_R values for the diallylamino, pyrrolidino, piperidino and perhydroazepino groups are not available). Quantum-chemical descriptors have long been used in QSAR studies [15]. A quantum chemical treatment of electronic effects is potentially more powerful than the Hammett-type approach since it allows greater flexibility in the construction of the data set. Thus, MO calculations were made. To simplify the computational problem, the calculations were made on model compounds consisting of only one of the two substituted pyridinium moieties and in which the spacer between the two charged nitrogen atoms was replaced by a methyl group. There is inherent error associated with the assumptions required to facilitate the calculations. In using quantum chemistry-based descriptors with a series of related compounds, the computational error is considered to be approximately constant throughout the series; thus, relative values of calculated descriptors can be meaningful even though their absolute values are not directly applicable [16]. The low-energy conformations obtained served as initial geometries for ab initio quantum chemical calcula-

tions. The structures of the model compounds are given in *table II*. Emphasis was placed on both accuracy and computational feasibility. While the highest accuracy is always desirable, computational accessibility is necessary. The *ab initio* (6-31G* level) calculations indicated deficiency of a negative charge on hydrogens atoms and excess charge on carbon and particularly on nitrogen atoms. The charge is, therefore, distributed according to the electronegativity of atoms. These results do not conform with our traditional beliefs, particularly in the case of quarternized species, which habitually assume that deficiency of a charge occurs on the nitrogen atom to which the chain is attached. According to the theoretical predictions the carbon and nitrogen atoms form a negatively charged core surrounded by a positively charged layer holding hydrogen atoms. Similar features have been predicted for several protonated nitrogen organic bases [17]. The partial charges on the ring N atom of the pyridinium moiety are shown in *table II*.

As can be seen from Eq. (1) there is a good correlation between $p(\text{IC}_{50})_{\text{ex vivo}}$ and the partial charge on the ring N atom of the pyridinium fragment:

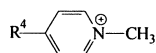
$$p(\text{IC}_{50})_{\text{ex vivo}} = -3.82 (\pm 1.74) - 13.4 (\pm 2.81) (\text{N}^1 \text{ charge}) \quad (1)$$

$$n = 10, r = -0.860, s = 0.220, F_{1,8} = 22.8, P < 0.005$$

where $p\text{IC}_{50} = -\log \text{IC}_{50}$, bearing in mind that the higher the value of $p\text{IC}_{50}$ the more potent is the compound, n is the number of compounds (compounds **1–5** and **7–11** are included), r is the correlation coefficient, s is the standard deviation, the numbers in brackets are standard errors of estimate and F is the F ratio between the variances of observed and calculated activities.

Eq. (1) shows that the more negative the partial charge on N^1 , the more potent is the compound. The influence of the variation of N^1 charge on the inhibitory potency of ChoK of the analogues is in agreement with the ^{13}C chemical shifts (in CD_3OD) of the methylene group bearing the endocyclic pyri-

Table II. Partial charges, frontier orbital and calculated solvation-free energies for model compounds used for correlation Eqs. (1)–(6)



Compound ^a	R ⁴	N ¹ charge	E _{HOMO} ^b	E _{LUMO} ^b	ΔG _{solv} ^c (kcal/mol)	p(IC ₅₀) _{ex vivo} ^d	p(IC ₅₀) _{antiprol} ^d
1a	–NMe ₂	–0.640	–296.7	–30.62	–45.01	4.77	5.70
2a	–NH ₂	–0.639	–315.4	–36.77	–54.84	4.64	5.40
3a	–CH ₂ OH	–0.596	–338.4	–55.03	–54.72	4.00	^e
4a	–CH ₃	–0.598	–341.0	–56.41	–49.80	4.00	4.70
5a	–COOH	–0.583	–346.4	–78.69	–64.99	3.86	^f
6a	–C≡N	–0.588	–357.7	–88.26	–62.90	^f	3.70
7a	–N(Allyl) ₂	–0.639	–285.1	–27.92	–46.21	4.77	6.26
8a	–NC ₄ H ₈ ^g	–0.642	–293.2	–28.61	–43.05	4.70	6.00
9a	–NC ₅ H ₁₀ ^h	–0.642	–290.0	–26.17	–44.73	5.02	6.40
10a	–NC ₆ H ₁₂ ⁱ	–0.641	–290.8	–27.36	–43.61	4.82	6.40
11a	–H	–0.586	–344.6	–63.50	–53.01	4.51	4.22

^a Model compound numbers correspond to the compound numbers of *table I*.

^b In kcal/mol.

^c Solvation-free energies were calculated with the HF/6-31G* method using the IPCM model implemented in GAUSSIAN94 [24]. The solvent used in the *ab initio* calculations was water at 298 K, with dielectric constant: 78.36.

^d All values are the means of two independent determinations performed in duplicate; $p\text{IC}_{50} = -\log \text{IC}_{50}$; the $p\text{IC}_{50}$ of the corresponding bispyridinium compound of *table I* is given for simplicity.

^e It cannot be accurately calculated because $\text{IC}_{50} > 100 \mu\text{M}$.

^f It cannot be accurately calculated because $\text{IC}_{50} > 1000 \mu\text{M}$.

^g Pyrrolidino.

^h Piperidino.

ⁱ Perhydroazepino.

dinium nitrogen atom of the symmetrical bisquaternary molecules **1–5** and **7–10** [18]. The more electron-releasing R^4 is, the more electron density is fed into the ring and the more positive charge is withdrawn from it; accordingly, the electron-donor groups shift the methylene resonance upfield. As a result, the negative charge on N^1 is increased, and so is potency. Obviously, the opposite holds for electron-withdrawing groups. Eq. (1) suggests that substituents that tend to donate electrons to the pyridinium ring make more potent inhibitors.

In principle, the previous reasoning seems contradictory: a simple electrostatic interaction between the quaternized nitrogen atom and an anionic group in the active site of ChoK should be increased with electron-withdrawing groups at position 4 of the symmetrical bispyridinium compounds. Such atomic charges are suitable for characterizing interactions according to classical point-charge electrostatic model. The electrostatic interaction may involve matching parts of the electric fields of the two interacting species, which have opposite signs, rather than matching point charges. For a better understanding of the experimental results, the energies of the HOMO (highest occupied molecular orbital, a measure of the ease of electron loss) and LUMO (lowest unoccupied molecular orbital, a measure of the ease of electron gain) of the compounds were calculated.

The energies of the frontier orbitals for the model compounds are also shown in *table II*. Normally, the spectroscopic transition energies are expressed in electron volts (eV) while the relative energies are expressed in kcal mol⁻¹. However, the frontier orbital energies (HOMO and LUMO) will be expressed in kcal mol⁻¹ as Eq. (4) (see later) correlates E_{LUMO} and solvation-free energy (G_{solv}). The inhibitory potency of ChoK of the analogues correlates well with the energy of the lowest unoccupied molecular orbital (E_{LUMO}) (Eq. (2)) and with the energy of the highest occupied molecular orbital (E_{HOMO}) (Eq. (3)):

$$p(\text{IC}_{50})_{\text{ex vivo}} = 5.33 (\pm 0.17) + 0.02 (\pm 0.00) E_{\text{LUMO}} \quad (2)$$

$$n = 10, r = 0.878, s = 0.207, F_{1,8} = 26.83, P < 0.001$$

$$p(\text{IC}_{50})_{\text{ex vivo}} = 8.83 (\pm 0.85) + 0.01 (\pm 0.00) E_{\text{HOMO}} \quad (3)$$

$$n = 10, r = 0.874, s = 0.210, F_{1,8} = 25.81, P < 0.001$$

In any thorough investigation of substituent effects, it is essential to prove that one's conclusions are *both* statistically valid *and* make chemical sense. Neither approach is sufficient alone [19]. It is appropriate to attempt to obtain insight into the physical meaning of the above-mentioned correlations 1, 2 and 3. This may suggest which of the three electronic parameters (N^1 charge, E_{LUMO} and E_{HOMO} , which are clearly themselves colinear, as shown explicitly by Eq. (5) is more consistent to use.

The physical meaning of the correlation with N^1 charge was not clear at this stage. Nevertheless, the involvement of electronic factors suggests the occurrence of either charge transfer or dipolar interactions. The transfer of a pair of electrons from the HOMO to the LUMO is, by definition, a reaction between a Lewis acid and a Lewis base. The compound that reacts via its HOMO is functioning as an electron-pair donor, that is, a Lewis base or a nucleophile. A nucleophile, or Lewis base, participates in reactions via its HOMO. The compound that reacts via its LUMO is functioning as an electron-pair acceptor, that is, a Lewis acid or an electrophile. An electrophile, or Lewis acid, participates in reactions via the LUMO.

With the exception of the hydrogen cation, H^+ , which has no electrons and cannot have a HOMO, all molecules and ions possess both a HOMO and a LUMO. Therefore there are always, in principle, two possible HOMO–LUMO combinations for reactions in which H^+ is not a participant. Fortunately, one of these combinations is usually obviously right and the other is usually obviously wrong.

It seems that in the E_{HOMO} and E_{LUMO} correlations, the higher the energies of the HOMO or the LUMO are (i.e. get closer to zero), the more potent the compound. If HOMO is considered to contribute at the level of interaction of the compound with ChoK, it follows that the compound acts as an electron donor, with the enzyme acting as an 'electron sink'. Fundamental chemical concepts are in discordance with this because these compounds are electron deficient and could not act as electron donors. It is therefore difficult to attribute a chemical meaning to the E_{HOMO} correlation.

4.1. Solvation of the model compounds

However, if LUMO is assumed to contribute at the level of interaction of the compound with ChoK, it is

necessary to consider the possibility of the formation of a charge transfer interaction with the latter, with the consequent interaction of the HOMO of ChoK (HOMO_{ChoK}) with the LUMO of the compound (LUMO_{compd}). With the solvent (H₂O) molecules acting as electron donors, the bispyridinium compounds could act as electron acceptors. The increase of the E_{LUMO} of the molecule would result in its weaker solvation, and thus, a stronger interaction with ChoK. A possible chemical meaning for the E_{LUMO} correlation is therefore offered by the hypothesis that a higher value for E_{LUMO} indicates a weaker solvation of the compound. A fact that strongly supports the solvation hypothesis has already been used by Galanakis et al. to explain the K⁺ channel blocking activity of dequalinium analogues [20]. Thus net ion–ion interactions are greatly reduced on hydration and only the consequent liberation of solvent molecules may create a significant entropy effect and favourable interaction [21]. Very recently, Miller et al. [22] have suggested that water can significantly enhance the electronic coupling between a donor and an acceptor in aqueous electron transfer processes.

The Hartree–Fock (HF) and the isodensity surface polarized continuum model (IPCM) [23] implemented in the GAUSSIAN94 [24] package were used to calculate absolute aqueous solvation-free energies (kcal mol^{−1}) because it has been shown that HF/IPCM gave the best balance between computational accessibility and accuracy between experimental and calculated values for pyridinium ions [25]. Both the active site of ChoK and the compounds would solvate but the different interactions between both species would depend on the nature of the R⁴ group of the pyridinium model compounds, since the solvation of ChoK is always the same. As can be seen from *table II*, the model compounds with higher E_{LUMO} (**7a**, **8a**, **9a** and **10a**) show a decreased free solvation energy, whereas those with lower E_{LUMO} have a higher G_{solv} (**5a** and **6a**). The unsubstituted compound (R⁴ = H) represents the intermediate case with an E_{LUMO} of −63.50 kcal mol^{−1} and an G_{solv} of −53.01 kcal mol^{−1}. There is a fairly good correlation between the E_{LUMO} and the free solvation energies of the model compounds (Eq. (4)), whereas there is a much better correlation between E_{LUMO} and the partial charge on N¹ of the pyridinium moiety (Eq. (5)):

$$E_{\text{LUMO}} = 74.9 (\pm 23.4) + 2.36 (\pm 0.46) G_{\text{solv}} \quad (4)$$

$$n = 10, r = 0.874, s = 9.66, F_{1,8} = 26.02, P < 0.001$$

$$E_{\text{LUMO}} = -20.7 (\pm 2.30) - 30.3 (\pm 2.71) (\text{N}^1 \text{ charge}) \quad (5)$$

$$n = 10, r = 0.970, s = 0.211, F_{1,8} = 125.26, P < 0.001$$

4.2. Relationship between antiproliferative activity and E_{LUMO}

Finally, as the main goal of this research is to search for new anticancer agents, the correlation between the antiproliferative activity and the E_{LUMO} has been calculated and the result is excellent (Eq. (6)):

$$p(\text{IC}_{50})_{\text{antiprol}} = 7.32 (\pm 0.21) + 4.42 \times 10^{-2} (\pm 4.39 \times 10^{-3}) E_{\text{LUMO}} \quad (6)$$

$$n = 9, r = 0.967, s = 0.270, F_{1,7} = 101.85, P < 0.001$$

4.3. Relationship between ChoK inhibition and antiproliferative activity

All compounds (with the exception of **11a**) are more potent against the HT-29 cell line (in vitro assay) than against ChoK (ex vivo assay). The level of the enzyme inhibition needed to perform a proliferation inhibition is not known. In other words, there is not a direct mathematical relationship between $p(\text{IC}_{50})_{\text{antiprol}}$ and $p(\text{IC}_{50})_{\text{ex vivo}}$, the reason for this being that the inhibition level for the PCho production necessary to induce the proliferation inhibition is not known. What is known is that all the ChoK inhibitors produce this inhibitor effect on proliferation. Nevertheless, taken together, the data presented here could be interpreted by means of a different unknown mechanism. With regard to the specificity, the parameters so far analyzed are negative except for ChoK. The title compounds are specific for ChoK since no inhibitory effect was observed against the phosphorylation of endogenous substrates such as phosphatidylinositol 3'-kinase (PI3K), two of the most relevant enzymes involved in the regulation of phospholipid metabolism such as phospholipase D (PLD) and phosphatidylinositol–phospholipase C (PI–PLC) or the Raf/mitogen-activated protein kinase (MAPK) pathway [26]. Moreover, compounds **1–11** showed no intercalating activity on DNA.

5. Conclusions

The quantum-chemically derived descriptors have definite chemical meaning, and they have thus proved to be especially useful in the clarification of the intermolecular interaction mechanism determining the molecular property or chemical process under study. The fitting of the three-dimensional structure and the complementary surface properties of a drug to its binding site are conditions for its biological activity. Even in simple *ex vivo* systems, the surrounding water molecules compete to solvate the binding site and to the functional groups of the ligand, and this balance can modify affinity. LUMOs seem to be essential for both inhibition of ChoK and for antiproliferative activity. In spite of being considered rather small, the variation of substituents presented here have been proved to be of general applicability for further extensive structure–activity relationship studies within the bisquaternary heterocycles as ChoK inhibitors. The regressor E_{LUMO} under study is proving to be useful for the design principles of even more potent inhibitors of ChoK, the results of which will be presented elsewhere.

6. Experimental

6.1. Chemistry

All solvents were used dried and freshly distilled. All evaporations were carried out in vacuo with a rotary evaporator. Solutions were dried over MgSO_4 before concentration under reduced pressure. Analytical thin-layer chromatography (TLC) was done on Merck silicagel F-254 plates with detection with iodine, an UV lamp or by charring with dilute sulfuric acid, using mixtures of CH_2Cl_2 :MeOH (10:0.1) as developing solvent. All analytical samples were TLC homogeneous. For normal column chromatography Merck silica gel 60 was used with a particle size 0.063–0.200 mm (70–230 mesh ASTM). For flash chromatography Merck silica gel 60 was used with a particle size 0.040–0.063 mm (230–400 mesh ASTM). Melting points (mp) were obtained on an Electrothermal melting point apparatus and are uncorrected. Ultraviolet–visible (UV–vis) absorption spectra were recorded on a Spectronic Genesys 5 spectrophotometer. NMR spectra were recorded on a 400.1 MHz ^1H - and 100.03 MHz ^{13}C -NMR Bruker ARX 400, a 300.13 MHz ^1H - and 75.78 MHz ^{13}C -NMR

Bruker AM-300 spectrometers and chemical shifts are reported relative to the residual ^1H and ^{13}C signals of the deuterated solvent (CHCl_3 , δ 7.24 and 77.1 ppm; CD_2HOD , δ 3.31 and 49.9 ppm). Chemical shifts (δ) quoted in the case of multiplets were measured from the approximate centre. Signals are designated as follows: s, singlet; d, doublet; dd, doublet of doublets; ddt, double double triplet; pst, pseudotriplet; psq, pseudoquartet; m, multiplet. Coupling constants are expressed in hertz. High resolution liquid secondary ion mass spectra (HR LSIMS) were carried out on a VG AutoSpec Q high resolution mass spectrometer (Fisons Instruments). The compounds gave accurate mass spectra, having no extraneous peaks. Analyses indicated by the symbols of the elements or functions were within $\pm 0.4\%$ of the theoretical values. All compounds were dried at 40–50°C and 0.1 mmHg for 16 h, but many tenaciously held on to water which appears to be a solvate.

6.1.1. General procedure for compounds 1–11

4-Substituted pyridine (1.58 mmol), bis-*p*-(bromomethyl)biphenyl [12] (0.79 mmol), and butanone (50 mL) were heated at 100°C in a sealed tube. After filtration and thorough washing with butanone and CHCl_3 , the solid product was purified by crystallization from ethanol (or methanol in the case of **6**) by adding diethyl ether to turbidity. The m.p.s, crystallization solvent, UV spectral data (the λ_{max} and the extinction coefficient, ϵ) and yields of compounds 1–11 are presented in table I.

6.1.1.1. 1,1'-[1,2-Ethylenebis(benzene-1,4-diylmethylene)]bis[(4-dimethylamino)pyridinium] dibromide (**1**)

^1H -NMR (300.13 MHz, CD_3OD): δ 8.22 (d, $J_{2,3} = 7.9$, 4H, H-2), 7.29 (d, $J = 8.3$, 4H, H-3_{benz} and H-5_{benz}), 7.24 (d, $J = 8.3$, 4H, H-2_{benz} and H-6_{benz}), 7.00 (d, $J_{2,3} = 7.9$, 4H, H-3), 5.33 (s, 4H, CH_2N^+), 3.25 (s, 12H, CH_3), 2.91 (s, 4H, CH_2). ^{13}C -NMR (75.57 MHz, CD_3OD): δ 158.00 (C-4), 144.13 (C-1_{benz}), 143.06 (C-2), 133.78 (C-4_{benz}), 130.56 (C-2_{benz} and C-6_{benz}), 129.46 (C-3_{benz} and C-5_{benz}), 109.11 (C-3), 61.54 (CH_2N^+), 40.39 (CH_3), 38.30 (CH_2). HR LSIMS (thioglycerol) Calc. m/z for $\text{C}_{30}\text{H}_{36}\text{N}_4\text{Br} [M-\text{Br}]^+$ 531.2123. Found m/z : 531.2130. Anal. $\text{C}_{30}\text{H}_{36}\text{N}_4\text{Br}_2 \cdot 2\text{H}_2\text{O}$ (C, H, N).

6.1.1.2. 1,1'-[1,2-Ethylenebis(benzene-1,4-diylmethylene)]bis(4-aminopyridinium) dibromide (**2**)

^1H -NMR (300.13 MHz, CD_3OD): δ 8.15 (d, $J_{2,3} = 7.6$, 4H, H-2), 7.28 (d, $J = 8.4$, 4H, H-3_{benz} and H-5_{benz}),

7.23 (d, $J = 8.4$, 4H, H-2_{benz} and H-6_{benz}), 6.86 (d, $J_{2,3} = 7.9$, 4H, H-3), 5.29 (s, 4H, CH₂N⁺), 2.91 (s, 4H, CH₂). ¹³C-NMR (75.57 MHz, CD₃OD): δ 160.82 (C-4), 144.12 (C-1_{benz}), 144.00 (C-2), 133.74 (C-4_{benz}), 130.59 (C-2_{benz} and C-6_{benz}), 129.41 (C-3_{benz} and C-5_{benz}), 110.95 (C-3), 61.80 (CH₂N⁺), 38.29 (CH₂). HR LSIMS (thioglycerol) Calc. m/z for C₂₆H₂₇N₄ [M–BrH–Br]⁺ 395.2236. Found m/z : 395.2234. Anal. C₂₆H₂₈N₄Br₂·0.2H₂O (C, H, N).

6.1.1.3. 1,1'-[1,2-Ethylenebis(benzene-1,4-diylmethylene)]bis[(4-hydroxymethyl)pyridinium] dibromide (3)

¹H-NMR (300.13 MHz, CD₃OD): δ 8.96 (d, $J_{2,3} = 6.9$, 4H, H-2), 8.07 (d, $J_{2,3} = 6.9$, 4H, H-3), 7.41 (d, $J = 8.2$, H-3_{benz} and H-5_{benz}), 7.27 (d, $J = 8.2$, 4H, H-2_{benz} and H-6_{benz}), 5.78 (s, 4H, CH₂N⁺), 4.92 (s, 4H, CH₂OH), 2.93 (s, 4H, CH₂). ¹³C-NMR (75.57 MHz, CD₃OD): δ 165.21 (C-4), 145.16 (C-2), 144.79 (C-1_{benz}), 132.45 (C-4_{benz}), 130.82 (C-2_{benz} and C-6_{benz}), 130.15 (C-3_{benz} and C-5_{benz}), 126.05 (C-3), 64.79 (CH₂N⁺), 62.86 (CH₂OH), 38.17 (CH₂). HR LSIMS (thioglycerol) Calc. m/z for C₂₈H₃₀N₂O₂Br [M–Br]⁺ 505.1491. Found m/z : 505.1493. Anal. C₂₈H₃₀N₂O₂Br₂ (C, H, N).

6.1.1.4. 1,1'-[1,2-Ethylenebis(benzene-1,4-diylmethylene)]bis(4-methylpyridinium) dibromide (4)

¹H-NMR (300.13 MHz, CD₃OD): δ 8.88 (d, $J_{2,3} = 6.6$, 4H, H-2), 7.94 (d, $J_{2,3} = 6.6$, 4H, H-3), 7.41 (d, $J = 8.2$, H-3_{benz} and H-5_{benz}), 7.27 (d, $J = 8.2$, 4H, H-2_{benz} and H-6_{benz}), 5.75 (s, 4H, CH₂N⁺), 2.93 (s, 4H, CH₂), 2.67 (s, 6H, CH₃). ¹³C-NMR (75.57 MHz, CD₃OD): δ 161.75 (C-4), 144.79 (C-2), 132.50 (C-4_{benz}), 130.81 (C-2_{benz} and C-6_{benz}), 130.15 (C-3_{benz} and C-5_{benz}), 130.10 (C-3), 64.63 (CH₂N⁺), 38.21 (CH₂), 22.03 (CH₃). HR LSIMS (thioglycerol) Calc. m/z for C₂₈H₃₀N₂Br [M–Br]⁺ 473.1592. Found m/z : 473.1578. Anal. C₂₈H₃₀N₂Br₂·H₂O (C, H, N).

6.1.1.5. 1,1'-[1,2-Ethylenebis(benzene-1,4-diylmethylene)]bis(4-carboxypyridinium) dibromide (5)

¹H-NMR (400.13 MHz, CD₃OD): δ 9.24 (d, $J_{2,3} = 6.6$, 4H, H-2), 8.54 (d, $J_{2,3} = 6.6$, 4H, H-3), 7.47 (d, $J = 8.1$, H-3_{benz} and H-5_{benz}), 7.31 (d, $J = 8.1$, 4H, H-2_{benz} and H-6_{benz}), 5.91 (s, 4H, CH₂N⁺), 2.94 (s, 4H, CH₂). ¹³C-NMR (100.62 MHz, CD₃OD): δ 147.11 (C-2), 145.09 (C-1_{benz}), 131.85 (C-4_{benz}), 130.93 (C-2_{benz} and C-6_{benz}), 130.52 (C-3_{benz} and C-5_{benz}), 129.10 (C-3), 65.83 (CH₂N⁺), 38.15 (CH₂). HR LSIMS (thioglycerol) Calc.

m/z for C₂₈H₂₅N₂O₄ [M–BrH–Br]⁺ 453.1814. Found m/z : 453.1817. Anal. C₂₈H₂₆N₂O₄Br₂ (C, H, N).

6.1.1.6. 1,1'-[1,2-Ethylenebis(benzene-1,4-diylmethylene)]bis(4-cyanopyridinium) dibromide (6)

¹H-NMR (400.13 MHz, CD₃OD): δ 9.32 (d, $J_{2,3} = 6.7$, 4H, H-2), 8.52 (d, $J_{2,3} = 6.7$, 4H, H-3), 7.46 (d, $J = 8.1$, H-3_{benz} and H-5_{benz}), 7.33 (d, $J = 8.1$, 4H, H-2_{benz} and H-6_{benz}), 5.91 (s, 4H, CH₂N⁺), 2.45 (s, 4H, CH₂). ¹³C-NMR (100.62 MHz, CD₃OD): δ 147.33 (C-2), 145.40 (C-1_{benz}), 132.49 (C-3), 131.30 (C-4_{benz}), 130.99 (C-2_{benz} and C-6_{benz}), 130.73 (C-3_{benz} and C-5_{benz}), 115.16 (CN), 66.49 (CH₂N⁺), 38.15 (CH₂). HR LSIMS (thioglycerol+H⁺) Calc. m/z for C₂₈H₂₅N₄ [M–2Br+H]⁺ 417.2079. Found m/z : 417.2075. Anal. C₂₈H₂₄N₄Br₂·0.3H₂O (C, H, N).

6.1.1.7. 1,1'-[1,2-Ethylenebis(benzene-1,4-diylmethylene)]bis[(4-diallylamino)pyridinium] dibromide (7)

¹H-NMR (400.13 MHz, CD₃OD): δ 8.26 (d, $J_{2,3} = 7.9$, 4H, H-2), 7.31 (d, $J = 8.2$, 4H, H-3_{benz} and H-5_{benz}), 7.25 (d, $J = 8.2$, 4H, H-2_{benz} and H-6_{benz}), 7.03 (d, $J_{2,3} = 7.9$, 4H, H-3), 5.90 (ddt, $J = 17.2$, 10.4 and 4.9, 4H, H-2_{allyl}), 5.35 (s, 4H, CH₂N⁺), 5.28 (ddt, $J = 10.4$, 1.2 and 1.1, 4H, H-3_{allyl}), 5.21 (ddt, $J = 17.2$, 1.2 and 1.1, 4H, H-3'_{allyl}), 4.24 (dt, $J = 4.9$ and 1.2, 8H, H-1_{allyl}), 2.91 (s, 4H, CH₂). ¹³C-NMR (100.62 MHz, CD₃OD): δ 157.89 (C-4), 144.25 (C-1_{benz}), 143.50 (C-2), 133.56 (C-4_{benz}), 131.49 (C-2_{allyl}), 130.59 (C-2_{benz} and C-6_{benz}), 129.57 (C-3_{benz} and C-5_{benz}), 118.38 (C-3_{allyl}), 109.92 (C-3), 61.78 (CH₂N⁺), 54.24 (C-1_{allyl}), 38.28 (CH₂). HR LSIMS (thioglycerol) Calc. m/z for C₃₈H₄₄N₄Br [M–Br]⁺ 635.2749. Found m/z : 635.2747. Anal. C₃₈H₄₄N₄Br₂·H₂O (C, H, N).

6.1.1.8. 1,1'-[1,2-Ethylenebis(benzene-1,4-diylmethylene)]bis(4-pyrrolidino)pyridinium) dibromide (8)

¹H-NMR (400.13 MHz, CD₃OD): δ 8.20 (d, $J_{2,3} = 7.6$, 4H, H-2), 7.29 (d, $J = 8.1$, 4H, H-3_{benz} and H-5_{benz}), 7.23 (d, $J = 8.1$, 4H, H-2_{benz} and H-6_{benz}), 6.86 (d, $J_{2,3} = 7.6$, 4H, H-3), 5.32 (s, 4H, CH₂N⁺), 3.55 (pst, $J = 6.8$, 8H, H-2_{pyrrolid} and H-5_{pyrrolid}), 2.90 (s, 4H, CH₂), 2.11 (psq, $J = 6.8$, 8H, H-3_{pyrrolid} and H-4_{pyrrolid}). ¹³C-NMR (100.62 MHz, CD₃OD): δ 155.14 (C-4), 144.08 (C-1_{benz}), 142.99 (C-2), 133.92 (C-4_{benz}), 130.55 (C-2_{benz} and C-6_{benz}), 129.43 (C-3_{benz} and C-5_{benz}), 109.70 (C-3), 61.55 (CH₂N⁺), 49.74 (C-2_{pyrrolid} and C-5_{pyrrolid}), 38.33 (CH₂), 26.14 (C-3_{pyrrolid} and C-4_{pyrrolid}).

HR LSIMS (thioglycerol) Calc. m/z for $C_{34}H_{40}N_4Br$ $[M-Br]^+$ 583.2436. Found m/z : 583.2438. Anal. $C_{34}H_{40}N_4Br_2 \cdot 2H_2O$ (C, H, N).

6.1.1.9. 1,1'-[1,2-Ethylenebis(benzene-1,4-diylmethylene)]bis(4-piperidino)pyridinium dibromide (9)

1H -NMR (300.13 MHz, CD_3OD): δ 8.17 (d, $J_{2,3} = 7.9$, 4H, H-2), 7.32 (d, $J = 8.2$, 4H, H-3_{benz} and H-5_{benz}), 7.26 (d, $J = 8.2$, 4H, H-2_{benz} and H-6_{benz}), 7.12 (d, $J_{2,3} = 7.9$, 4H, H-3), 5.30 (s, 4H, CH_2N^+), 3.70 (t, $J = 6.8$, 8H, H-2_{piperid} and H-6_{piperid}), 2.91 (s, 4H, CH_2), 1.75 (m, 12H, H-3_{piperid}, H-4_{piperid} and H-5_{piperid}). ^{13}C -NMR (75.57 MHz, CD_3OD): 156.85 (C-4), 144.13 (C-1_{benz}), 143.49 (C-2), 133.76 (C-4_{benz}), 130.56 (C-2_{benz} and C-6_{benz}), 129.47 (C-3_{benz} and C-5_{benz}), 109.27 (C-3), 61.38 (CH_2N^+), 49.10 (C-2_{piperid} and C-6_{piperid}), 38.32 (CH_2), 26.67 (C-3_{piperid} and C-5_{piperid}), 24.93 (C-4_{piperid}). HR LSIMS (thioglycerol) Calc. m/z for $C_{36}H_{44}N_4Br$ $[M-Br]^+$ 611.2749. Found m/z : 611.2773. Anal. $C_{36}H_{44}N_4Br_2 \cdot 2.4H_2O$ (C, H, N).

6.1.1.10. 1,1'-[1,2-Ethylenebis(benzene-1,4-diylmethylene)]bis(4-perhydroazepino)pyridinium dibromide (10)

1H -NMR (300.13 MHz, CD_3OD): δ 8.20 (d, $J_{2,3} = 7.9$, 4H, H-2), 7.31 (d, $J = 8.2$, 4H, H-3_{benz} and H-5_{benz}), 7.25 (d, $J = 8.2$, 4H, H-2_{benz} and H-6_{benz}), 7.05 (d, $J_{2,3} = 7.9$, 4H, H-3), 5.32 (s, 4H, CH_2N^+), 3.72 (t, $J = 6.8$, 8H, H-2_{perhydroazep} and H-7_{perhydroazep}), 2.91 (s, 4H, CH_2), 1.85 (m, 8H, H-3_{perhydroazep} and H-6_{perhydroazep}), 1.60 (m, 8H, H-4_{perhydroazep} and H-5_{perhydroazep}). ^{13}C -NMR (75.57 MHz, CD_3OD): δ 157.19 (C-4), 144.17 (C-1_{benz}), 143.33 (C-2), 133.75 (C-4_{benz}), 130.57 (C-2_{benz} and C-6_{benz}), 129.51 (C-3_{benz} and C-5_{benz}), 109.01 (C-3), 61.48 (CH_2N^+), 51.33 (C-2_{perhydroazep} and C-7_{perhydroazep}), 38.33 (CH_2), 27.34 (C-3_{perhydroazep}, C-4_{perhydroazep}, C-5_{perhydroazep} and C-6_{perhydroazep}). HR LSIMS (thioglycerol) Calc. m/z for $C_{38}H_{48}N_4Br$ $[M-Br]^+$ 639.3062. Found m/z : 639.3050. Anal. $C_{38}H_{48}N_4Br_2 \cdot 1.8H_2O$ (C, H, N).

6.1.1.11. 1,1'-[1,2-Ethylenebis(benzene-1,4-diylmethylene)]bispyridiniumdibromide (11)

1H -NMR (300.13 MHz, CD_3OD): δ 9.08 (d, $J_{2,3} = 6.6$, 4H, H-2), 8.62 (t, 2H, H-4), 8.14 (pst, 4H, H-3), 7.43 (d, $J = 8.2$, 4H, H-3_{benz} and H-5_{benz}), 7.29 (d, $J = 8.2$, 4H, H-2_{benz} and H-6_{benz}), 5.83 (s, 4H, CH_2N^+), 2.94 (s, 4H, CH_2). ^{13}C -NMR (75.57 MHz, CD_3OD): δ 147.27 (C-2), 145.90 (C-4), 144.94 (C-1_{benz}), 132.27 (C-4_{benz}), 130.87 (C-2_{benz} and C-6_{benz}), 130.28 (C-3_{benz} and

C-5_{benz}), 129.72 (C-3), 65.52 (CH_2N^+), 38.19 (CH_2). HR LSIMS (thioglycerol) Calc. m/z for $C_{26}H_{26}N_2Br$ $[M-Br]^+$ 445.1279. Found m/z : 445.1275. Anal. $C_{26}H_{26}N_2Br_2 \cdot 1.5H_2O$ (C, H, N).

6.1.2. 4-Chloropyridine

4-Chloropyridine hydrochloride (10 g) was dissolved in water (20 mL), and excess 6 N NaOH was added to the solution to reach a pH of 12. The 4-chloropyridine formed an organic layer above the aqueous phase. The mixture was extracted with diethyl ether (4×50 mL). The combined ether extracts were dried ($MgSO_4$), filtered and concentrated in vacuo, and the remaining dark brown liquid was kept at high vacuum for 20 min (6.42 g, 86%).

6.1.3. General procedure for the synthesis of 4-(diallylamino)- and 4-(cycloamino)pyridines

4-Chloropyridine (38 mmol) was refluxed with excess of the amine (95 mmol) under an argon atmosphere for 3 days. The mixture was neutralized with 1 N NaOH, extracted with diethyl ether (4×100 mL), dried ($MgSO_4$), filtered and rotaevaporated off. This residue was purified by flash chromatography using the mixture $Cl_3CH:MeOH$, 9:1 as eluant, giving the title compound.

6.1.3.1. 4-(Diallylamino)pyridine

Following the general procedure (Section 6.1.3) and using diallylamine, 4-(diallylamino)pyridine was prepared in 34.5% yield as a dark brown viscous liquid; TLC ($Cl_3CH:MeOH$, 8.5:1.5) R_f : 0.43. 1H -NMR (300.13 MHz, CD_3OD): δ 8.09 (d, $J_{2,3} = 7.3$, 2H, H-2_{pyr}), 6.84 (d, $J_{2,3} = 7.3$, 2H, H-3_{pyr}), 5.89 (ddt, $J_{2,3'} = 17.2$, $J_{2,3} = 10.1$, $J_{1,2} = 4.7$, 2H, H-2_{allyl}), 5.24 (ddt, $J_{2,3} = 10.1$, $J_{3,3'} = 1.5$, $J_{1,3} = 1.7$, 2H, H-3_{allyl}), 5.18 (ddt, $J_{2,3'} = 17.2$, $J_{3,3'} = 1.5$, $J_{1,3'} = 1.7$, 2H, H-3'_{allyl}), 4.13 (dt, $J_{1,2} = 4.7$, $J_{1,3} = 1.7$, $J_{1,3'} = 1.7$, 4H, H-1_{allyl}). ^{13}C -NMR (75.57 MHz, CD_3OD): δ 157.32 (C-4_{pyr}), 144.56 (C-2_{pyr}), 132.49 (C-2_{allyl}), 117.53 (C-3_{allyl}), 108.69 (C-3_{pyr}), 53.57 (C-1_{allyl}). Anal. $C_{11}H_{14}N_2$ (C, H, N).

6.1.3.2. 4-Piperidinopyridine

Yield: 95%; m.p. 78–79°C (lit.¹⁴ m.p.: 80°C); TLC ($Cl_3CH:MeOH$, 1:1) R_f : 0.41. 1H -NMR (300.13 MHz, $CDCl_3$): δ 8.17 (d, $J_{2,3} = 6.6$, 2H, H-2_{pyr}), 6.63 (d, $J_{2,3} = 6.6$, 2H, H-3_{pyr}), 3.33 (t, 4H, H-2_{piperid} and H-6_{piperid}), 1.63 (m, 6H, H-3_{piperid} and 4_{piperid}). ^{13}C -NMR (75.57 MHz, $CDCl_3$): δ 155.11 (C-4_{pyr}), 148.88 (C-2_{pyr}), 108.10 (C-3_{pyr}), 47.25 (C-2_{piperid} and C-6_{piperid}), 25.13 (C-3_{piperid} and C-5_{piperid}), 24.28 (C-4_{piperid}).

6.1.3.3. 4-(Perhydroazepino)pyridine

Yield: 89%; TLC ($\text{Cl}_3\text{CH}:\text{MeOH}$, 1:1) R_f : 0.43. ^1H -NMR (300.13 MHz, CDCl_3): δ 8.12 (d, $J_{2,3} = 6.7$, 2H, H-2_{pyr}), 6.44 (d, $J_{2,3} = 6.7$, 2H, H-3_{pyr}), 3.41 (t, 4H, H-2_{perhydroazep} and H-7_{perhydroazep}), 1.73 (m, 4H, H-3_{perhydroazep} and H-6_{perhydroazep}), 1.49 (m, 4H, H-4_{perhydroazep} and H-5_{perhydroazep}). ^{13}C -NMR (75.57 MHz, CDCl_3): δ 153.23 (C-4_{pyr}), 149.39 (C-2_{pyr}), 106.16 (C-3_{pyr}), 48.61 (C-2_{perhydroazep} and C-7_{perhydroazep}), 27.03 (C-3_{perhydroazep} and C-6_{perhydroazep}), 26.76 (C-4_{perhydroazep} and C-5_{perhydroazep}). Anal. $\text{C}_{11}\text{H}_{16}\text{N}_2$ (C, H, N).

6.1.4. Computational methods

Molecular modelling and preliminary geometry optimizations were performed using SYBYL software package. Then the structures were reoptimized using semiempirical quantum chemical calculations with the semiempirical AM1 (Austin Model 1) method [27], previous to their treatment by the ab initio methods. The AM1 method [27] was used because indicated that the ring N atom carries a negative partial charge (data not shown). Gas-phase geometry optimizations were performed via ab initio quantum mechanical methods. Ab initio calculations were performed using GAUSSIAN-94 [24] with the 6-31G* basis set. Geometry optimizations were performed at the Hartree–Fock (HF) level of theory.

Free energies of solvation in aqueous solution were calculated using the isodensity surface polarized continuum model (IPCM) [23]. The IPCM is implemented in the GAUSSIAN-94 [24] package. All solvation calculations were performed on the gas-phase optimized structures. Due to the pyridinium ring, the presence of solvent is not expected to have a significant influence on the optimized geometries, as was verified in several tests (not described). For ab initio reaction-field calculations the dielectric of water was set to 78.36 and the isodensity cutoff values were 0.001 a.u. Solvation-free energies in aqueous solution were obtained as the difference between the HF/6-31G* gas-phase energies and the corresponding energies of the same level of theory with the IPCM solvation model.

Statistical analysis of the relationships between ChoK inhibitory or antiproliferative activities and substituent properties of interest was performed by partial least-squares algorithm using the QSAR module of SYBYL software [28].

6.2. Pharmacology

The ex vivo ChoK inhibition and antiproliferative assays against HT-29 cells were followed in accordance with the protocols reported previously [9, 10].

Acknowledgements

We thank the Spanish CICYT (project SAF98-0112-C02-01) for financial support. The award of a grant from the Junta de Andalucía to M.C.N. and Dr. Ali Haidour for recording the ^1H - and ^{13}C -NMR spectra are gratefully acknowledged. We also want to thank one of the referees for the helpful comments given.

References

- [1] Kennedy E.P., Fed. Proc. 20 (1961) 934–940.
- [2] Kent C., Prog. Lipid Res. 29 (1990) 87–105.
- [3] Vance D.E., Biochem. Cell Biol. 68 (1990) 1151–1165.
- [4] Barbacid M., Ann. Rev. Biochem. 56 (1987) 779–827.
- [5] Abdellatif M., MacLellan W.R., Schneider M.D., J. Biol. Chem. 269 (1994) 15423–15426.
- [6] Barbacid M., Eur. J. Clin. Invest. 20 (1990) 225–235.
- [7] Wiesmüller L., Wittinghofer F., Cell. Signal. 6 (1994) 247–267.
- [8] Bhakoo K.K., Williams S.R., Florian C.L., Land H., Noble M.D., Cancer Res. 56 (1996) 4630–4635.
- [9] Hernández-Alcoceba R., Saniger L., Campos J., Núñez M.C., Khaless F., Gallo M.A., Espinosa A., Lacal J.C., Oncogene 15 (1997) 2289–2301.
- [10] Hernández-Alcoceba R., Fernández F., Lacal J.C., Cancer Res. 59 (1999) 3112–3118.
- [11] Hansch C., Leo A., Substituent Constants for Correlation Analysis in Chemistry and Biology, Wiley, New York, 1979, pp. 1–8.
- [12] Cram D.J., Steinberg H., J. Am. Chem. Soc. 73 (1951) 5691–5704.
- [13] Vaidya R.A., Mathias L., J. Am. Chem. Soc. 108 (1986) 5514–5520.
- [14] Jerchel D., Jakob L., Chem. Ber. 91 (1958) 1266–1273.
- [15] Karelson M., Lobanov V.S., Katritzky A.R., Chem. Rev. 96 (1996) 1027–1043.
- [16] Redl G., Cramer R.D. III, Berkoff C.E., Chem. Soc. Rev. 3 (1974) 273–292.
- [17] Lubkowski J., Blazejowski J., J. Phys. Chem. 95 (1991) 2311–2316.
- [18] Campos J., Núñez M.C., Rodríguez V., Gallo M.A., Espinosa A., Bioorg. Med. Chem. Lett. 10 (2000) 767–770.
- [19] Reynolds W.F., Gomes A., Maron A., MacIntyre D.W., Tanin A., Can. J. Chem. 61 (1983) 2376–2384.
- [20] Galanakis D., Calder J.A.D., Ganellin C.R., Owen C.S., Dunn P.M., J. Med. Chem. 38 (1995) 3536–3546.

- [21] Davies R.H., Timms D., in: Smith H.J. (Ed.), *Introduction to the Principles of Drug Design and Action*, Harwood Academic Publishers, Amsterdam, 1998, pp. 51–96.
- [22] Miller N.E., Wander M.C., Cave R.J., *J. Phys. Chem. A* 103 (1999) 1084–1093.
- [23] Foresman J.B., Keith T.A., Wiberg K.B., Snoonian J., Frisch M.J., *J. Phys. Chem.* 100 (1996) 16098–16104.
- [24] GAUSSIAN-94; Revision C.2, M.J. Frisch, G.W. Trucks, H.B. Schlegel, P.M.W. Gill, B.G. Johnson, M.A. Robb, J.R. Cheeseman, T. Keith, G.A. Petersson, J.A. Montgomery, K. Raghavachari, M.A. Al-Laham, V.G. Zakrzewski, J.V. Ortiz, J.B. Foresman, J. Cioslowski, B.B. Stefanov, A. Nanayakkara, M. Challacombe, C.Y. Peng, P.Y. Ayala, W. Chen, M.W. Wong, J.L. Andres, E.S. Replogle, R. Gomperts, R.L. Martin, D.J. Fox, J.S. Binkley, D.J. Defrees, J. Baker, J.P. Stewart, M. Head-Gordon, C. Gonzalez, J.A. Pople, Gaussian Inc., Pittsburgh, PA, 1995.
- [25] Chen I.-J., MacKerell A.D. Jr, *Theor. Chem. Acc.* 103 (1999) 483–494.
- [26] To know the molecular mechanisms of signal transduction, see: C.-H. Heldin, M. Purton (Eds.), *Signal Transduction*, Chapman and Hall, London, 1996.
- [27] Dewar M.J.S., Zoebish E.G., Healy E.F., Stewart J.J.P., *J. Am. Chem. Soc.* 107 (1985) 3902–3909.
- [28] SYBYL, version 6.5, Tripos Associates, St. Louis, MO, 1998.